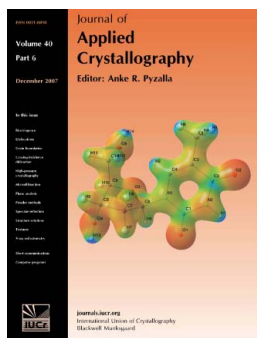


## A full-pattern fitting algorithm for energy-dispersive X-ray diffraction

Yu-Hui Dong, Jing Liu, Yan-Chun Li and Xiao-Dong Li

*J. Appl. Cryst.* (2003). **36**, 1123–1127

This is the ORIGINAL ARTICLE, which was replaced in August 2008 to correct a problem with figure numbering.



Many research topics in condensed matter research, materials science and the life sciences make use of crystallographic methods to study crystalline and non-crystalline matter with neutrons, X-rays and electrons. Articles published in the *Journal of Applied Crystallography* focus on these methods and their use in identifying structural and diffusion-controlled phase transformations, structure–property relationships, structural changes of defects, interfaces and surfaces, *etc.* Developments of instrumentation and crystallographic apparatus, theory and interpretation, numerical analysis and other related subjects are also covered. The journal is the primary place where crystallographic computer program information is published.

Crystallography Journals **Online** is available from [journals.iucr.org](http://journals.iucr.org)

# A full-pattern fitting algorithm for energy-dispersive X-ray diffraction

Yu-Hui Dong,\* Jing Liu, Yan-Chun Li and Xiao-Dong Li

Beijing Synchrotron Radiation Facility (BSRF), Institute of High Energy Physics (IHEP), Chinese Academy of Science (CAS), PO Box 918 (2-7), Beijing 100039, People's Republic of China.

Correspondence e-mail: dongyh@ihep.ac.cn

Received 22 August 2002

Accepted 6 June 2003

A full-pattern fitting algorithm for energy-dispersive X-ray diffraction is proposed, especially for high-pressure X-ray diffraction studies. The algorithm takes into account the errors in measuring the energy and the diffraction angle. A lognormal function is introduced to represent the background. All the peaks that are detectable in the diffraction spectra, including fluorescence and diffraction peaks, are considered together. Because all the data points in the spectra are used, the accuracy of the cell parameters obtained by this method is very high. This is very helpful in the analysis of the equation of state and the identification of new phases under high pressure.

© 2003 International Union of Crystallography  
Printed in Great Britain – all rights reserved

## 1. Introduction

In recent years, the properties of materials under high pressure have attracted many researchers. High pressure provides another dimension for the phase diagram. Some new materials may only be synthesized under high pressure. High pressure combined with high temperature is very important in geoscience because it is a good way to simulate the condition of the mantle and even the core of the Earth.

X-ray diffraction is a very important technique for structure determination. The diamond anvil cell (DAC) is a widely used technique for obtaining pressures higher than 100 GPa. Since the sample inside the DAC is very small, energy-dispersive X-ray diffraction, with the aid of synchrotron radiation, becomes a useful tool in this research. However, the diffraction signal is still very weak and the background scattering in this kind of experiment is quite high. A suitable method of data processing becomes necessary.

The developments in X-ray diffraction analysis have followed from neutron diffraction. Many methods, especially the Rietveld method, which represents a milestone in structure refinement, and related software have been published (Rietveld, 1969; Young, 1995; Langford, 1992; Langford & Louer, 1996; Pawley, 1981; Le Bail *et al.*, 1988). However, these improvements mainly focus on the angle-dispersive mode. Still little software can deal with the data of an energy-dispersive experiment. Some examples are *GSAS* (Larson & Von Dreele, 1985), *RIETICA* (Hunter & Howard, 1998) and *XRDA* (Desgreniers & Lagarec, 1998). *GSAS* is a powerful tool for Rietveld refinement, which can also deal with 'native' energy-dispersive data, or angle-dispersive data converted from energy-dispersive data (Ballirano & Caminiti, 2001). The special features of energy-dispersive diffraction, such as the fluorescence peaks, which always appear (but never occur in the angle-dispersive mode), and the high background due to the scattering of the diamond cell, the gasket materials and the

pressure-transmitting medium, as well as the error in the measured energy are not considered appropriately by software such as *GSAS* and *XRDA*. In this paper, an algorithm of full-pattern fitting for energy-dispersive X-ray diffraction is proposed.

Compared with other software, such as *GSAS*, *RIETICA* and *XRDA*, the method we propose here has some new features. (i) The background is presented as the sum of a lognormal function and a polynomial. Since the background due to the scattering of diamond and the gasket material, as well as the pressure-transmitting medium, is always asymmetric, it is found that a lognormal function is suitable for representing it. Only few parameters are used for the background and a good result is achieved. Less parameters in the fitting yields a more reliable result. (ii) The fluorescence peaks are considered together with the diffraction peaks, even though these peaks usually appear on the lower energy side and one can just simply cut the spectra to avoid the interference of fluorescence. The latter approach is quite reasonable when the energy range of measurement can reach 70 keV, or even 100 keV, since most fluorescence appears below 20 keV. However, when the energy cannot reach very high, *e.g.* 40 keV, it is better to consider the fluorescence peaks. (iii) The calibration of energy measured by a solid-state detector with a multichannel analyser is considered carefully over the entire energy range, especially the possible non-linearity of the response of the detector over the range. This effect should be small but can affect the result markedly.

## 2. Algorithm

The wavelength of a diffraction peak in energy-dispersive X-ray diffraction is given by the Bragg condition:

$$\lambda = 2d \sin \theta, \quad (1)$$

where  $\lambda$  is the wavelength of diffraction,  $d$  is the interplanar spacing of this diffraction and  $\theta$  the diffraction angle. The corresponding energy should be

$$E = 12.398/\lambda, \quad (2)$$

where the energy  $E$  is in keV and the wavelength  $\lambda$  is in Å. Usually in a real spectrum of an energy-dispersive diffraction experiment, not only the diffraction peaks, but also the fluorescence peaks from the sample can be observed. The energies of the fluorescence peaks are fixed and only dependent on the elements in the sample, while the positions of the diffraction peaks are connected with the crystalline structure of the sample and the diffraction angle  $\theta$ . The detector used in collecting the spectra is a solid-state detector with a multi-channel analyser. The energy measured by the detector is usually calibrated by some radiation source and fluorescence, such as  $^{55}\text{Fe}$  (5.894, 6.489 keV), Pt (9.4423, 11.0707 keV), Au (9.713, 11.4423 keV), Mo (17.47934, 19.6083 keV), Ag (22.1629, 24.9424 keV), *etc.* Because only few points in the total energy range are used, the accuracy of the calibration should not be very high. The value of  $\theta$  is calculated according to the positions of the diffraction peaks of some standard samples, such as Au, Pt and Ag, which are also used as the internal standard for the measurement of pressure. Since the energy measured is not very accurate, the error in  $\theta$  can be very high. The result of these errors is that the accuracy of the obtained structural parameters is quite low.

Naturally, one way to avoid the problem is to consider all the possible factors together in a full-pattern fitting. Especially under ambient pressure, since the energies of the fluorescence peaks and the interplanar spacing of the standard sample are well known, we can calibrate the energy carefully over the entire energy range, as well as the diffraction angle  $\theta$ . With the calibration, the interplanar spacing under pressure can be obtained very accurately.

The real value of the energy and that measured by the solid-state detector can be related by the following formula:

$$E_{\text{real}} = E_{\text{exp}} + E_0 + E_1 E_{\text{exp}} + E_2 E_{\text{exp}}^2. \quad (3)$$

$E_{\text{real}}$  is the real value of energy, while  $E_{\text{exp}}$  is the measured one. The energy shift ( $E_0$ ), linearity ( $E_1$ ) and the non-linearity ( $E_2$ ) of the solid-state detector are considered together.

The full spectrum  $y(E_i)$  can be expressed by the sum of the background  $b(E_i)$  and the composition of a series of peaks  $h_j(E_i)$ :

$$y(E_i) = b(E_i) + \sum_j h_j(E_i), \quad (4)$$

where  $E_i$  is the energy of every point in the spectrum, and  $j$  is the number of peaks (including the fluorescence and diffraction peaks).

The background  $b(E_i)$  is represented by the sum of a polynomial and a lognormal function. In traditional angle-dispersive powder diffraction, the background is usually represented by a polynomial (Young, 1995). Some other types of background functions are used, such as the Chebyshev polynomial and cosine Fourier series in *GSAS* (Larson & Von

Dreele, 1985), the  $1/x$  function in *TOPAS* (Bruker AXS, 2000), *etc.* In energy-dispersive diffraction inside a DAC, the pressure-transmitting medium, the diamond and the gasket give rise to a strong scattering background, which is usually asymmetric. The lognormal function is suitable for expressing this kind of background since it is also asymmetric. Three parameters only are enough to represent the lognormal function. Fewer parameters used in the fitting means that the fitting is more reliable.

The profiles of all the peaks are considered using as a pseudo-Voigt (pV) function. The profiles of the fluorescence peaks from the sample are Lorentzian, while the solid-state detector would give a Gaussian expansion; the measured peaks are the convolution of these two functions, a Voigt function. In order to save calculation time, we chose a pV function to express these profiles. Furthermore, the profiles of the diffraction peaks can be expressed very well by a pV function because a pV function is quite good in expressing the profiles of diffraction peaks in the angle-dispersive mode (Langford & Louer, 1996). The conversion from the energy scale to the angle scale can be treated as linear in a short range, so a pV function should represent the profile of energy-dispersive diffraction very well.

The maximum intensities, widths and mixing parameters of the pV functions are fitting parameters. The positions of the diffraction peaks are decided by the crystalline structure of the sample and the calibration of energy, as well as the diffraction angle  $\theta$ . The widths and mixing parameters of all the diffraction peaks are treated as fitting parameters in the program because they are quite difficult to ascertain otherwise, owing to the complicated nature of the mechanism of peak broadening, such as the axial divergences, the size of the grain in the sample, the density and type of defects, *etc.* (Langford & Wilson, 1978; Wilkens, 1969, 1970; Warren, 1969). The process for diffraction peaks is the Pawley method (Pawley, 1981), *i.e.* to refine the cell parameters with cell constraints, while other methods are based on the Rietveld refinement or the Le Bail method. For the fluorescence peaks, the positions are decided by the calibration of energy, and their widths and mixing parameters are also treated as fitting parameters. All the maximum intensities of the peaks are proportional to the intensity of the incident synchrotron radiation at the energies of the peak positions and dependent on the absorption of diamond and the gasket. It is convenient to treat them as fitting parameters as well. A non-linear least-squares fitting engine based on the Levenberg–Marquardt algorithm (Garbow *et al.*, 1996) is used.

The program (*HPXRD*) is freely available for academic use.

### 3. Experiment

The experiments were carried out at the high-pressure station of BSRF (Beijing Synchrotron Radiation Facility), beamline 3W1A. The beamline provides a white beam with energy 5–40 keV. A diamond anvil cell with a culet of 0.5 mm diameter is used for creating the high pressure. Samples are held in a

**Table 1**  
The values of the parameters for energy calibration and  $2\theta$ .

	$E_0$ (keV)	$E_1$	$E_2$	$2\theta$ ( $^\circ$ )
Value	-0.0864	0.01392	-0.000488	17.83638
Error	0.0015	0.00018	0.000005	0.00069

**Table 2**  
The values of the cell parameters and volumes under pressure.

$P$ (GPa)	$a_{Pt}$ ( $\text{\AA}$ )	$a_{B_2}$ ( $\text{\AA}$ )	$c_{B_2}$ ( $\text{\AA}$ )	$V_{B_2}$ ( $\text{\AA}^3$ )	$a_{B_1}$ ( $\text{\AA}$ )	$V_{B_1}$ ( $\text{\AA}^3$ )
0	3.923	3.2473 (2)	5.2036 (4)	95.039		
6.1	3.89489 (8)	3.2134 (2)	5.1382 (6)	91.895		
8.3	3.88558 (8)	3.2002 (7)	5.129 (2)	90.978	4.2190 (2)	75.098
11.6	3.87251 (9)				4.2074 (1)	74.482
18.3	3.8477 (1)				4.17133 (20)	72.581
29.5	3.81154 (10)				4.1177 (2)	69.818
37.5	3.7887 (1)				4.08247 (20)	68.041

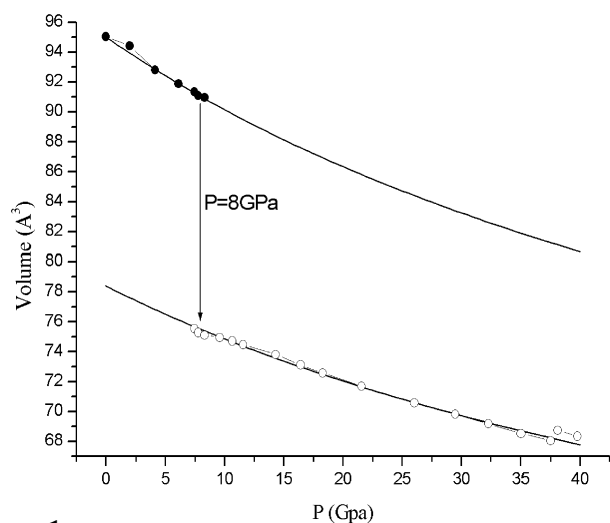


**Figure 1**  
The difference in energy between the measured and the real energy. The maximum error is 230 eV.

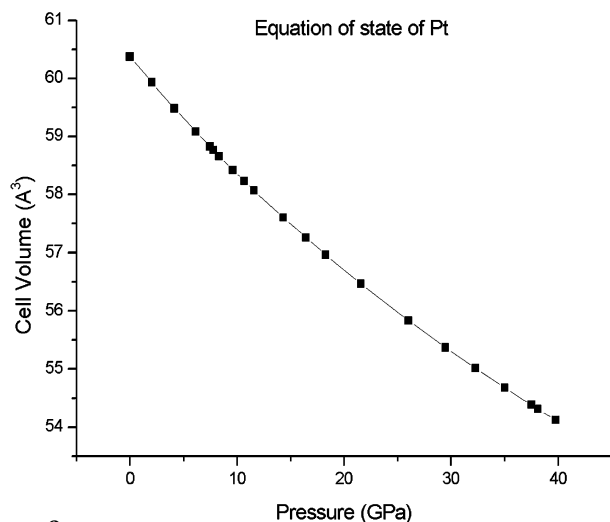


**Figure 2**  
The fitting result of ZnO+Pt under ambient pressure. The fitting result is reported (line) together with the experimental data (dots) and the residual (line). The residual is very small; it shows that both the modelling of peaks by the  $pV$  function and the background are correct.

gasket with a 0.2 mm hole. A solid-state Ge detector with multichannel analyser is used to collect the diffraction spectra.

ZnO samples were used in the work reported in this paper. Pt powder was mixed with the sample in order to calibrate the pressure because the equation of state of Pt is well known.

#### 4. Results and discussion

The usual routine for processing the data is to fit the pattern under ambient pressure first, in order to obtain the correct values of  $2\theta$  and energy calibration. This is very important for the next step because a very small error of these values would affect the total analysis markedly. Because the cell parameters of Pt are known very precisely, this step can be completed with quite high accuracy. Table 1 lists the values we obtained from the ZnO+Pt sample under ambient pressure. The errors of all values are quite small.

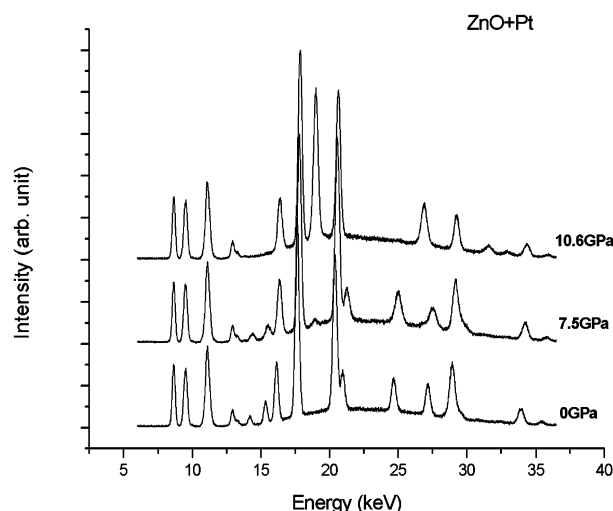


**Figure 3**  
The background of the spectrum in Fig. 2, clearly showing the asymmetry of the background.

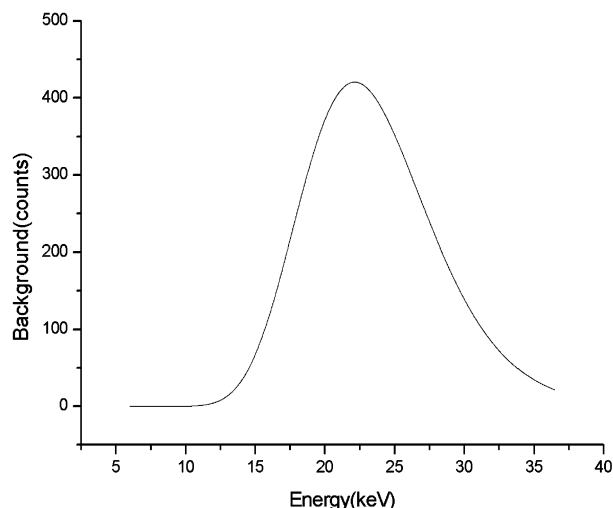


**Figure 4**  
A selection of spectra of ZnO under different pressures. A phase transition occurs at about 8 GPa.

The cell parameters for ZnO obtained under ambient pressure are  $a = b = 3.2473 (2) \text{ \AA}$ ,  $c = 5.2036 (4) \text{ \AA}$ , which are very close to the values reported elsewhere (Gerward & Olsen, 1995). The difference in energy between the measured and real energy is very small, as shown in Fig. 1. The maximum error of energy is about 230 eV. This value seems small but affects the calculation of the cell parameters considerably. This is because when the difference in energy of two diffraction peaks is several keV's, as is usually the case, e.g. 5 keV, the error in the cell parameters would be of the order of  $0.23/5 = 4.6\%$  if we do not correct the error in energy carefully. The error can be larger when more peaks are detected because the distance between the peaks becomes small. The error in the interplanar spacing can affect the indexing of an unknown phase markedly; in turn, indexing is of utmost importance in determining an unknown crystal structure.

In the processing of the spectra under pressure, the values of the energy calibration and  $2\theta$  are fixed and we can fit the cell parameters. Some values of the cell parameters under different pressures are listed in Table 2. The errors are very small. Since all the possible factors affecting the peak positions have been taken into account and all the data points in the spectra are used, the accuracy of the interplanar spacing, as well as of the cell parameters, is very high. This is the merit of full-pattern fitting.

Some fitting results are presented in Fig. 2. The residuals are quite small. This indicates that the pV functions we use here to represent the peak profiles are correct. The background is shown in Fig. 3, which clearly shows asymmetry.

It is reported that ZnO undergoes a phase transition under pressure at about 10 GPa. The structure changes from hexagonal (B4 wurtzite) to cubic (B1 rocksalt) (Gerward & Olsen, 1995; Karzel *et al.*, 1996). Fig. 4 shows several spectra under different pressures. The pressures are calculated with respect to the cell parameters of Pt according to the equation of state, which is displayed in Fig. 5. The equation of state of ZnO is shown in Fig. 6. For the B4 and B1 phases, the bulk modulus

and its pressure derivatives can be obtained from these data according to the Murnaghan equation. For the B4 phase, because there are not enough data points, the pressure derivative of the bulk modulus is fixed to the calculated value of 3.6 (Karzel *et al.*, 1996). The bulk modulus is 171 GPa. For the B1 phase, the bulk modulus obtained is 208 GPa and the pressure derivative is 4.3. It is very clear that a phase transition occurs at a pressure of about 8 GPa.

The cell parameter of cubic ZnO at the phase transition is about  $4.2190 \text{ \AA}$ . The cell volume collapses by about 18%. This value is in very good agreement with that reported elsewhere (Gerward & Olsen, 1995). The pressure of the transition, as well as the bulk modulus and its pressure derivatives, are close to the literature values (Gerward & Olsen, 1995). We suggest that the errors are related to the problem of measuring the pressure. Since the position of the sample can change during compression, the value of  $2\theta$  could change slightly. This is an unavoidable problem of this kind of method for measuring pressure. A method that is independent of the  $2\theta$  value would be much better, such as measuring the fluorescence peak shift of ruby.

## 5. Conclusion

A full-pattern fitting algorithm that takes into account the positions of all the fluorescence and diffraction peaks is presented. The errors in the measurement of the energy by a solid-state detector with a multichannel analyser and in the  $2\theta$  value are considered. All peaks are represented by a pV function. The strong and asymmetric background is modelled by a lognormal function and polynomial. Since all the data points of the spectra are considered, the accuracy of the analysis is improved. If some unknown phases are present, this method can give better interplanar spacings. This is very important for the indexing of the diffraction peaks of the unknown phase, which in turn is most important in structure

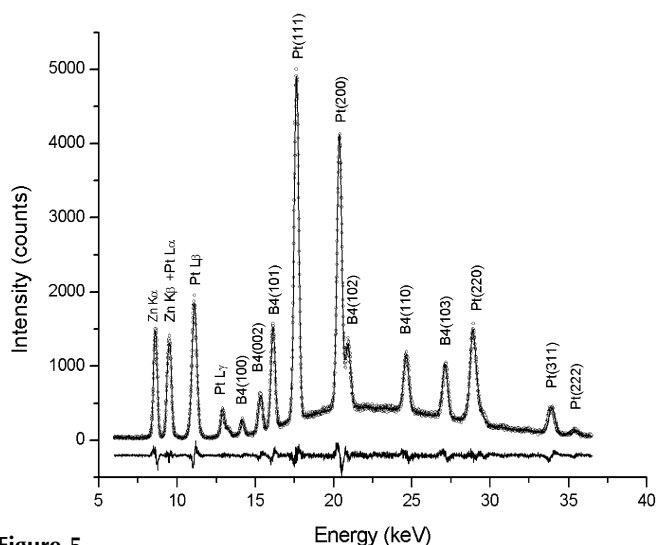


**Figure 5**  
The equation of state of Pt.

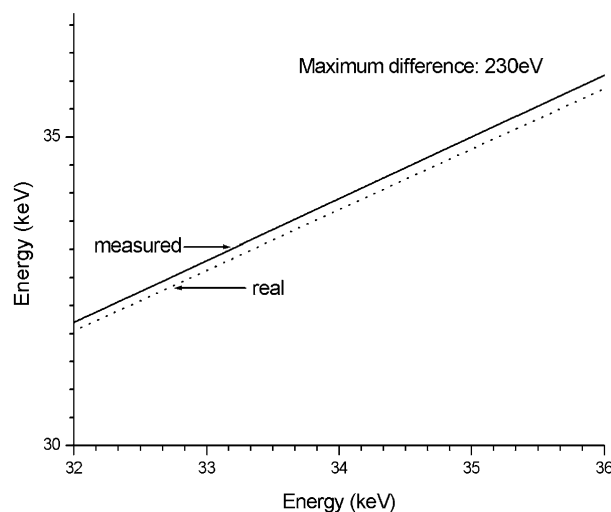


**Figure 6**  
The equation of state of ZnO. The fitting result of the Murnaghan equation (line) and the experimental data (dots) are plotted together.

analysis. This method was applied to ZnO and the results for the cell parameters are in very good agreement with the literature values. The pressure at which the phase transition occurs is 8 GPa, close to the value reported by others. The reasons for the errors in pressure at the phase transition, as well as in the bulk modulus and its pressure derivatives, lie in the method of pressure measurement employed in our experiments.

## References

- Ballirano, P. & Caminiti, R. (2001). *J. Appl. Cryst.* **34**, 757–762.
- Bruker AXS (2000). *TOPAS*, version 2.0, *User Manual*. Bruker AXS, Karlsruhe, Germany.
- Desgreniers, S. & Lagarec, K. (1998). *J. Appl. Cryst.* **31**, 109–110.
- Garbow, B. S., Hillstrom, K. E. & More, J. J. (1996). MINPACK Project. Argonne National Laboratory, November 1996 (<http://www.netlib.org/minpack>).
- Gerward, L. & Olsen, J. S. (1995). *J. Synchrotron Rad.* **2**, 233–235.
- Hunter, B. A. & Howard, C. J. (1998). *LHPM: a Computer Program for Rietveld Analysis of X-ray Neutron Powder Diffraction Pattern*. Lucas Height Research Laboratory, Australian Nuclear Science and Technology Organization, NSW, Australia.
- Karzel, H., Potzel, W., Kofferlein, M., Schiessl, W., Steiner, M., Hiller, U., Kalvius, G. M., Mitchell, D. W., Das, T. P., Blaha, P., Schwarz, K. & Pasternak, M. P. (1996). *Phys. Rev. B*, **53**, 11425–11438.
- Langford, J. I. (1992). *Accuracy in Powder Diffraction II, NIST Special Publication No. 846*, edited by E. Price & J. K. Stalick, pp. 110–126. Gaithersburg, MA: US Department of Commerce.
- Langford, J. I. & Louer, D. (1996). *Rep. Prog. Phys.* **59**, 131–234.
- Langford, J. I. & Wilson, A. J. C. (1978). *J. Appl. Cryst.* **11**, 102–113.
- Larson, A. C. & Von Dreele, R. (1985). *GSAS: General Structure Analysis System*, LAUR 86-748. Los Alamos National Laboratory, New Mexico, USA.
- Le Bail, A., Duroy, H. & Fourquet, J. L. (1988). *Mater. Res. Bull.* **23**, 447–452.
- Pawley, G. S. (1981). *J. Appl. Cryst.* **14**, 357–361.
- Rietveld, H. M. (1969). *J. Appl. Cryst.* **2**, 65–71.
- Warren, B. E. (1969). *X-ray Diffraction*. New York: Dover.
- Wilkens, M. (1969). *Acta Metall.* **17**, 1155–1159.
- Wilkens, M. (1970). *Phys. Status Solidi A*, **2**, 359–370.
- Young, R. A. (1995). Editor. *The Rietveld Method*. Oxford University Press.